applied optics

Programmable light source based on an echellogram of a supercontinuum laser

Ding Luo,[1,2,*] Miro Taphanel,[1,2] Thomas Längle,[2] and Jürgen Beyerer[1,2]

[1]Vision and Fusion Laboratory, Karlsruhe Institute of Technology, Karlsruhe 76131, Germany
[2]Fraunhofer Institute of Optronics, System Technologies and Image Exploitation, Karlsruhe 76131, Germany
*Corresponding author: ding.luo@kit.edu

Received 18 January 2017; revised 16 February 2017; accepted 16 February 2017; posted 16 February 2017 (Doc. ID 285062); published 10 March 2017

Illumination systems with tunable spectrums have been receiving an increasing amount of attention due to their wide application and unique capability. This paper proposes a programmable light source in the visible range based on the combination of a prism and an echelle grating. A supercontinuum laser is utilized as the primary source, whose echellogram is projected to a digital mirror device for wavelength selection. A complete calibration procedure is developed to generate any target spectrum of choice. Experiments have shown that spectral peaks with a full width at half-maximum of 1 nm can be easily generated and the wavelength tuning resolution can reach as small as 0.01 nm.

OCIS codes: (080.2740) Geometric optical design; (120.2440) Filters; (120.4820) Optical systems; (230.6080) Sources; (300.6320) Spectroscopy, high-resolution.

https://doi.org/10.1364/AO.56.002359

1. INTRODUCTION

The ability to modulate the spectrum of light serves as a powerful tool in various fields of research, such as biomedical optics, optical communication, hyperspectral imaging, optical measurement, etc. The variability of the spectrum in such systems enables various analog signal processing methods which greatly improves the performance and generates new possibilities. For example, Hirai *et al.* developed a multispectral image projector using a programmable spectral light source [1]. By using multiple primary colors, the system is capable of wide-gamut projection.

Earlier development of spectrum modulation was mainly driven by the need for wavelength division multiplexing (WDM) in optical communication as well as chemical analysis. Various technologies have been proposed and implemented to realize a tunable spectral filter, including acousto-optics [2–4], liquid crystals [5,6], fiber Bragg grating [7], interferometers [8], etc. These methods typically focus on the realization of tunable bandpass filters, some of which include tunable bandwidth. Nevertheless, they lack the capability of manipulating a complete spectrum.

With the wide popularity of commercial digital light processing (DLP) projectors, digital mirror devices (DMDs) have been receiving an increasing amount of attention for the development of novel optical systems. Riza and Sumriddetchkajorn introduced a digitally controlled multiwavelength programmable attenuator using a two-dimensional digital micromirror device [9]. Based on this concept, a broadband optical equalizer was developed later [10]. Chuang and Lo proposed a programmable light spectrum synthesis system which used collimated output from a single-mode fiber as the primary source [11]. The light is dispersed onto a DMD chip with a diffraction grating. One dimension of the DMD is used for wavelength selection, while the other dimension is used for intensity modulation of the corresponding wavelength. This concept has been commercialized using a xenon arc lamp as the primary source and a DMD for spectral filtering (OneLight Spectra by OneLight Corp. and OL-490 Agile Light Source by Optronic Laboratories). Although having been applied in surgical and biomedical research, these sources typically suffer from performance limitations due to the compromise between spectral resolution and efficiency. Wood and Elson proposed the use of a supercontinuum laser as the primary source coupled with a prism as the disperser and a DMD as the modulator to construct a tunable light source [12]. Diffraction analysis is made considering the DMD as a blazed grating. The system is capable of producing illumination bands with a roughly constant width of 6 nm.

With constant development of the DMD, the binary pattern rate has been increased over the years, allowing for real-time time multiplexing schemes to be developed. Therefore, instead of using only one dimension of the DMD for wavelength selection, this paper proposes a system which utilizes the complete two-dimensional area of the DMD for wavelength

selection in order to achieve superior spectral resolution, while intensity modulation is realized in a time multiplexing fashion. The system is designed and constructed based on the combination of orthogonally placed prism and echelle grating to generate the echellogram of a supercontinuum laser onto the DMD. The complete calibration procedure is developed and implemented. Several spectra are generated and analyzed, indicating a minimum full width at half-maximum (FWHM) of less than 1 nm. When acting as a scanning bandpass filter, the wavelength tuning resolution can reach as small as 0.01 nm. The proposed filtering system can be constructed with a relatively low cost and easily attached to commonly available supercontinuum lasers to generate illumination with a programmable spectrum.

2. SYSTEM DESIGN AND SIMULATION

A. Theoretical Background

Diffraction grating can be characterized with the grating equation [13]

$$d(\sin\theta_m + \sin\theta_i) = m\lambda, \tag{1}$$

where m stands for the diffraction order, λ represents the wavelength of the light, d represents the grating period, θ_i and θ_m represent the incidence angle and diffraction angle, respectively.

Echelle grating is a special type of blazed grating characterized by a large blazing angle of the grooves and used at high diffraction orders obtaining high dispersion. Since an echelle grating is typically installed in a Littrow configuration under the blazing condition, the angular dispersion can be written as

$$\frac{\partial\theta_m}{\partial\lambda} = \frac{m}{2d\cos\theta_m} = \frac{\tan\phi_b}{\lambda}, \tag{2}$$

where ϕ_b denotes the blazing angle.

Although the groove density of echelle grating is smaller than common blazed gratings, the groove structure is optimized for a much larger blazing angle and therefore the light is concentrated into much higher diffraction orders. As shown in Eq. (2), in a Littrow configuration under the blazing condition, the dispersion of the grating depends only on the blazing angle of the grating and the wavelength, which allows the echelle grating to have much higher dispersion than normal blazed grating.

The free spectral range $\Delta\lambda_{\mathrm{FSR}}$ defines the largest bandwidth in one order that does not overlap with the same bandwidth in adjacent orders,

$$\Delta\lambda_{\mathrm{FSR}} = \frac{\lambda_s}{m} = \frac{\lambda_l}{m+1}, \tag{3}$$

where λ_s and λ_l represent the shortest and longest wavelengths, respectively.

For an echelle grating, due to the large blazing angle, higher numbers of orders are utilized, which leads to a very small free spectral range in each order. This also means that multiple orders will overlap at the same diffraction angle, making it necessary to apply a secondary disperser in the orthogonal direction in order to separate the orders from each other. Such secondary dispersers, also known as cross dispersers, can be placed before or after the echelle grating.

B. Optical Design

The system is first treated as an echellogram system and designed in the sequential mode of OpticStudio. As illustrated in Fig. 1, the echellogram system is composed of five components. A supercontinuum laser serves as the light source of the system. The target wavelength ranges from 470 to 700 nm. The laser beam first enters an equilateral dispersion prism made of F2 glass to be dispersed in the horizontal direction. The incidence angle with respect to the normal of the prism surface is 39°. The output beam is immediately incident on an echelle grating in the Littrow configuration under the blazing angle for vertical dispersion. The echelle grating has a blazing angle of 63.5° and a grating period of 31.6 l pmm. Such combination of prism and echelle grating is chosen so that the echellogram covers the entire area of the DMD. Finally, the two-dimensionally dispersed light is focused onto the DMD through an achromatic doublet with a focal length of 100 mm.

To demonstrate the orthogonal dispersions generated by the two dispersers, Fig. 2 presents the footprint diagrams at two apertures: the echelle grating surface (left) and the first surface of the achromatic doublet after the echelle grating (right). Light with wavelengths of 468.1 nm and 472.1 nm at the 119th order and 697.6 nm and 706.6 nm at the 78th order is

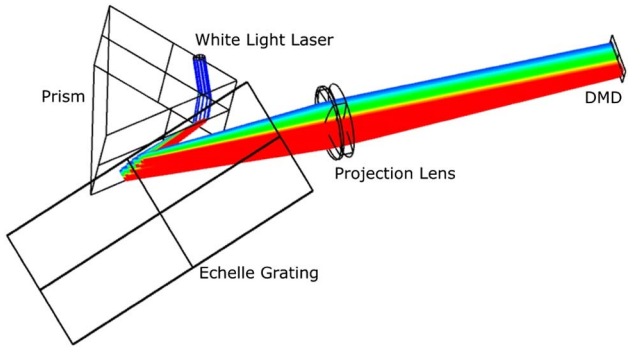

Fig. 1. System schematic of the echellogram system in sequential mode of OpticStudio.

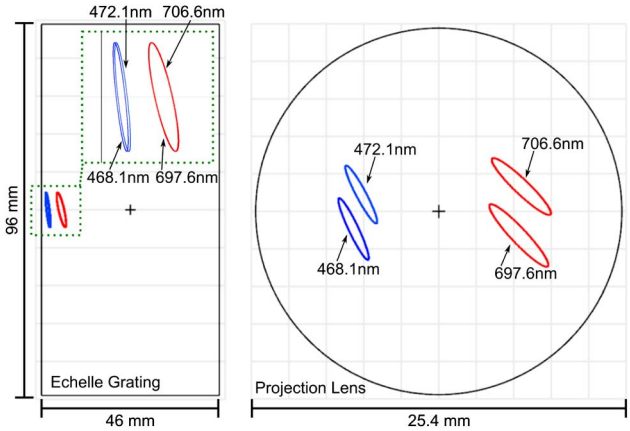

Fig. 2. Footprint diagrams of the 119th order (blue) and the 78th order (red). Left: before the echelle grating surface. The dotted green square shows a zoomed-in illustration. Right: after the echelle grating and before the achromatic doublet.

illustrated and colored by its respective wavelength. As can be seen on the left, after the prism and before the echelle grating, light is only dispersed in the horizontal direction. After the echelle grating, vertical dispersion is introduced as shown by the diagram on the right.

A program is written in Python with a PyZDDE [14] package to automate the computation of diffraction orders and the setting of multi-configuration. Totally, 42 configurations are utilized, each representing an order in the range from the 78th order to the 119th order. Within each order, 21 wavelengths are specified, equidistantly covering the free spectral range in that order. The system is telecentric and it has been optimized in terms of the spot size, which, with 4 mm size, is contained within the Airy disk, offering diffraction-limited optical quality. As an example, Fig. 3 illustrates the spot diagram of 558.6 nm at the 99th diffraction order.

To characterize the spectral resolution of each DMD pixel, the diffraction ensquared energy fraction is calculated for a specific position while varying the wavelength to generate the spectral response of the underlying pixel. The pixel is placed at the centroid of the focused spot at 558.6 nm. The pupil sampling resolution is specified as 512 × 512 and a wavelength range from 558.5 to 558.7 nm is investigated. The goal is to characterize the bandwidth of light falling on this particular pixel. As illustrated by Fig. 4, the spectral response of one pixel with a width of 7.6 μm has a FWHM of 0.065 nm. Although this value varies with respect to the wavelength, the order of magnitude remains the same. When a larger area of 10 × 10 pixels is investigated, the resulting spectral width is slightly increased to 0.108 nm. As the size of the airy disk is relatively large with respect to the DMD pixel, the diffraction effect is dominating the calculation of the ensquared energy fraction. This leads to the nonlinear increase of spectral width when the detector area is increased. Since these values represent the optimum situation in theory, the spectral widths will be further widened in practice due to inaccurate alignment and tolerances of the optics.

C. Zemax Simulation

Once the optimization is complete, the system is reimplemented in the nonsequential mode of OpticStudio to simulate the generation of the echellogram and the effect of the DMD. Each pixel of the DMD has two stable states, namely on and off, where the micro mirror is turned by +12° and −12°, respectively. Although the DMD in practice has 1920 × 1080 pixels, due to internal speed limitations of OpticStudio, the DMD used in simulation is set to 192 × 108 pixels. As illustrated in Fig. 5, several additional components are placed compared to the echellogram in the sequential mode. When the pixels of the DMD are turned on, a coupling lens is used to focus the reflected light into a liquid light guide. When the pixels of the DMD are turned off, the light is deflected into a beam trap. Therefore, by sending a specific pattern to the DMD, certain wavelength components can be selected and coupled into the light guide for further application.

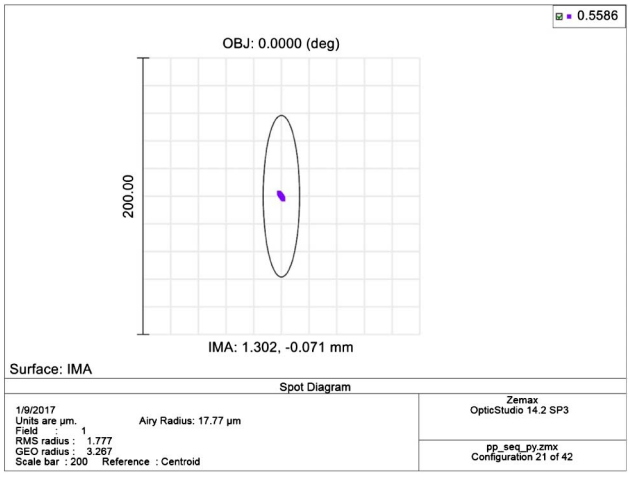

Fig. 3. Spot diagram of 558.6 nm at the 99th diffraction order.

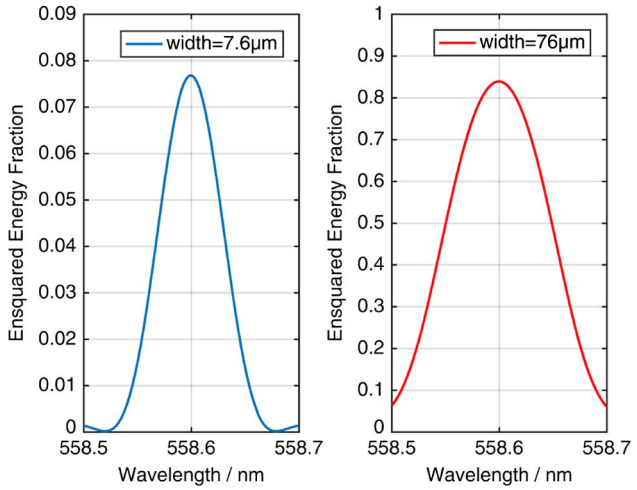

Fig. 4. Spectral resolution characterized by the diffraction ensquared energy. Left: calculated with one pixel. Right: calculated with a block size of 10 × 10 pixels.

Distribution of the light on the DMD is simulated through ray tracing in the nonsequential mode. Totally, 400 wavelengths are specified for each diffraction order and are divided into 20 groups. Ray tracing is conducted for each group with 40,000 rays. A detector color object with 1920 × 1080 pixels is placed right above the DMD to collect the projected rays. Another Python program is written to automate the switching between groups and orders. Figure 6 illustrates the simulation result.

A detector is placed at the focus of the coupling lens to investigate the intensity distribution at the entrance of the light guide. As shown in Fig. 7, when all pixels of the DMD are turned on, the reflected light forms an irregular spot through the coupling lens on the detector. In practice, a light guide with a diameter of 5 mm is utilized to collect as much light as possible, which is shown as the red circle in Fig. 7.

Two things should be noted regarding the design and simulation implemented in OpticStudio. First, the grating efficiency is not taken into consideration during the simulation. For each order, the energy is assumed to be distributed evenly within the free spectral range. In practice, according to the characteristics of the echelle grating, most of the energy will be concentrated around the blazing angle, i.e., within the free spectral

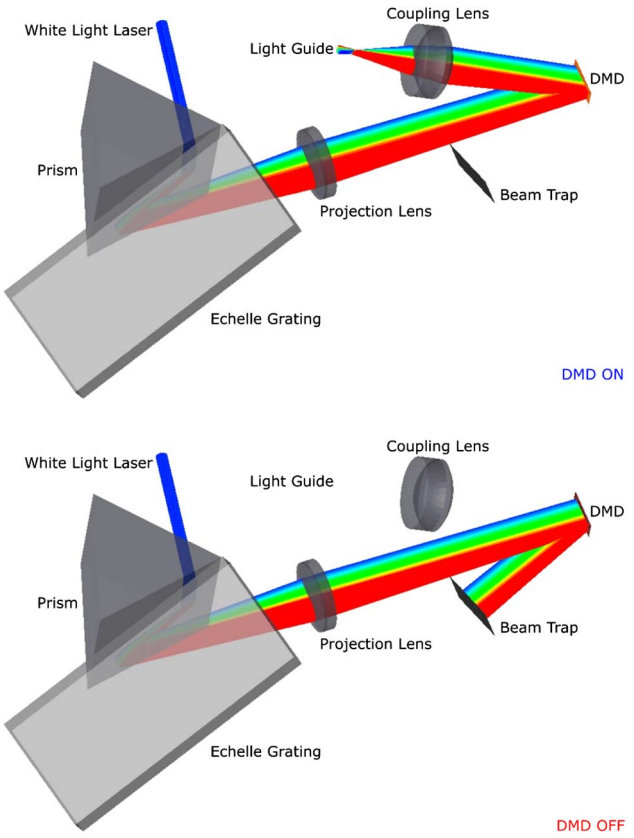

Fig. 5. System schematic of the programmable light source in nonsequential mode of OpticStudio. Upper: all pixels are on. Lower: all pixels are off.

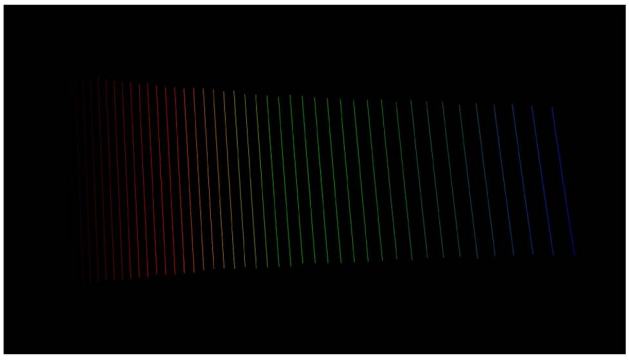

Fig. 6. Simulated echellogram upon the DMD chip based on nonsequential ray tracing.

range of each order. Nevertheless, a small portion of the energy will also spread to other directions, partly due to imperfect blazing facet structure. Second, only geometric ray tracing is conducted when investigating the interaction between light and the DMD. In reality, due to the small size of the DMD pixel, the diffraction effect cannot be ignored [12]. With its periodic structure, the DMD acts like a blazed grating with a switchable blazing angle, which generates multiple two-dimensional diffraction orders instead of simple reflection. Therefore, the

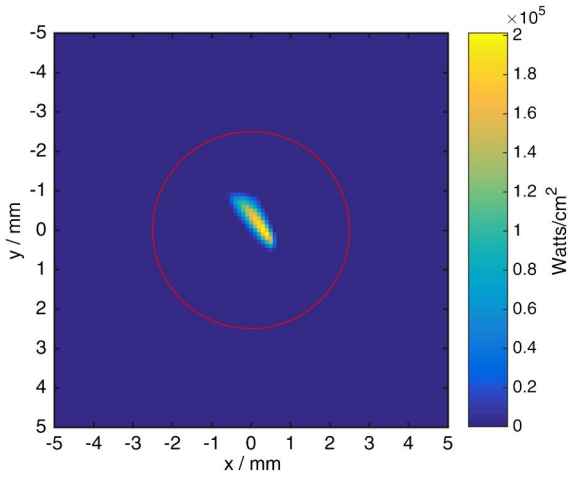

Fig. 7. Irradiance distribution at the entrance of the liquid light guide. The red circle indicates the aperture of the light guide, which has a diameter of 5 mm.

simulation of the intensity distribution in Fig. 7 is only a rough approximation of the real scenario.

3. SYSTEM SETUP AND ALIGNMENT

The primary light source in the system is an obsolete model of a supercontinuum laser from Koheras (now NKT Photonics). It is similar to the SuperK EXTREME EXW-12 model from NKT Photonics, which delivers 1.2 W of power in the range from 350 to 850 nm. As shown in Fig. 8, the collimated output of the supercontinuum laser is first expanded with a 4× reflective beam expander (BE04R/M from Thorlabs). The expanded beam then gets reflected by a visible mirror so that the infrared component passes through the mirror and enters a beam trap. The reflected beam passes through the prism and gets dispersed in the horizontal direction. As mentioned in the previous section, the echelle grating has a period of 31.6 lpmm and a blazing angle of 63.5°. The grating is manufactured by Richardson Grating Lab using Zerodur for substrate and aluminum for coating. After vertical dispersion generated by the echelle grating, the

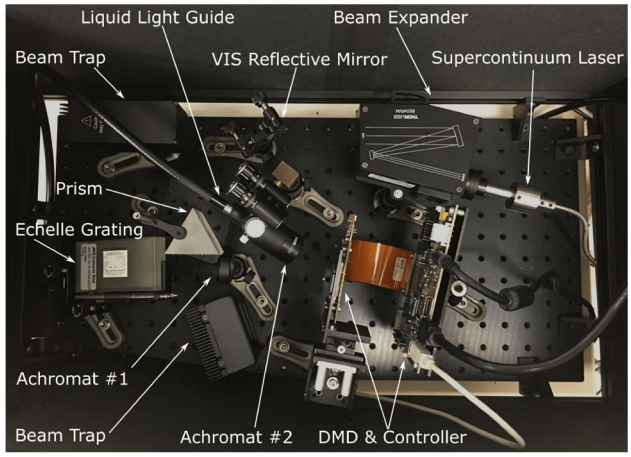

Fig. 8. System setup of the programmable light source within its encapsulation.

two-dimensionally dispersed light is focused onto the DMD with an achromatic doublet (AC254-100 from Thorlabs). The DMD used in the system is DLP LightCrafter 6500 EVM from Texas Instruments. The DMD chip has 1920 × 1080 pixels with a pitch of 7.6 μm. Light of wavelengths corresponding to pixels that are turned on is collected by a second achromatic doublet with shorter focal length (AC254-30 from Thorlabs) and coupled into a liquid light guide with a diameter of 5 mm. A second beam trap is placed in the opposite position to collect light with wavelengths corresponding to pixels that are turned off.

Although the system is composed of relatively few components, the alignment proves to be not trivial. To begin with, laser safety is a major issue throughout the alignment process. As a Class 4 laser, the supercontinuum laser utilized in the system is not eye safe even when operated at 1% of power. At earlier stage of calibration as well as under scenarios where higher power is required, an augmented reality setup based on Oculus Rift and a webcam is utilized. A Python program with OpenCV feeds the image from the webcam to the Oculus rift with proper distortion correction, in order to avoid any contact between the eyes of the operator and the laser. In other situations, a laser goggle with an IRD5 filter from NoIR LaserShields is used and an additional ND filter is applied to the laser. Once alignment is finished, the complete system is encapsulated with a cage made of anodized aluminum rails and black cardboard, so that the calibration can be made without further laser safety protection. In general, alignment with a supercontinuum laser is always difficult, since a proper laser goggle with sufficient filtering will render the environment and nonilluminating components too dark.

Second, as shown in Fig. 6, the positions of the prism and the echelle grating are designed so that usage of the DMD area is optimized. In practice, taking the grating efficiency into consideration, the incidence angle at the entrance of the prism has to be modified together with all following components to find the optimum. What adds to the complexity of alignment is that the spectrum varies with the power of the supercontinuum laser. In particular, shorter wavelengths gain more power as the total power is increased, due to the nonlinear effect of supercontinuum generation. As more subtle adjustments are made using a laser goggle as protection, which requires low power operation, room for shorter wavelengths can only be estimated and reserved. Since the complete measurement of the echellogram is only possible at the calibration stage, the circle of alignment and calibration has to be repeated several times before an optimum situation is found.

Third, although the prism and the grating are designed to be placed side by side, as shown in Fig. 5, the edge of the ruling area of the echelle grating exhibits lesser quality than the center area in practice, which may lead to deterioration of the signal-to-noise ratio in the final system. Therefore, the echelle grating is moved to the left of the prism to allow for the usage of the center area. Although angular positions of the orders remain the same, the spatial positions are more separated at the projection lens, which adds more spherical error to the edge orders. Such error is considered acceptable since the spot size is well below the diffraction limit, as shown in Fig. 3.

Last but not least, the DMD exhibits very strong diffraction effects, i.e., the reflection is composed of multiple two-dimensional orders. The rotation of the DMD and the position of the coupling lens has to be manipulated iteratively to have maximum collected power while maintaining acceptable spot size upon the DMD.

4. CALIBRATION AND RESULTS

A. Calibration Method

The calibration process aims to characterize the spectral response of each pixel so that any arbitrary spectrum can be generated by calculating the corresponding DMD pattern. As shown in Fig. 9, an additional setup is built outside of the encapsulated programmable light source. The liquid light guide is routed out of the encapsulation for calibration. Output light from this end of the liquid light guide is first collimated through an aspheric condenser lens (ACL5040U from Thorlabs), then passes through a pair of microlens arrays (#63-230 from Edmund Optics) for homogenization. Lastly, an achromatic doublet is used to project the light to a rectangular area, where a fiber is placed which leads to the spectrometer. A special mounting adaptor is machined in-house to hold all components at the correct positions. The combination of the condenser, the microlens arrays, and the achromat is selected to match the diameter and numerical aperture of the liquid light guide output, so that most of the energy is uniformly concentrated in a central rectangular block of 16 mm × 12 mm, with a minor portion of energy leaked to adjacent blocks. The homogenized rectangular illumination can be directly used in various applications once calibration is finished.

To make the calibration, first all DMD pixels are turned on. The position of the fiber end is aligned so that the overall intensity of the spectrum is largest. Then each pixel of the DMD is turned on while the corresponding spectrum is recorded. Due to limitation of the speed of the DMD, the signal-to-noise ratio of the spectrometer, and computer storage, instead of scanning all pixels individually, square blocks of pixels are grouped together to form macro pixels, which are scanned and measured in practice. The size of the block is chosen to be 5 × 5, in order to balance the calibration speed with resolution. The integration time of the spectrometer is set at 5 ms, and the average

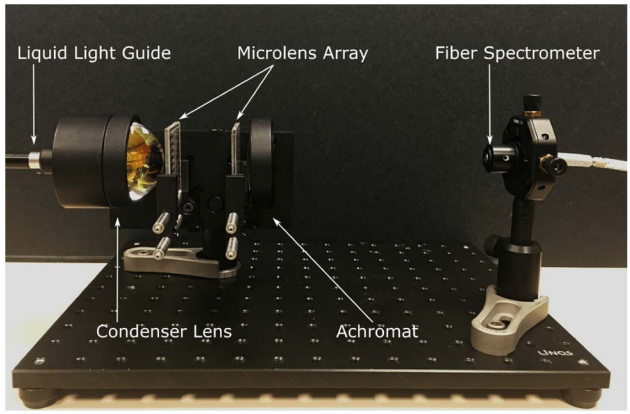

Fig. 9. Calibration setup with homogenized rectangular illumination area projected onto a fiber leading to the spectrometer.

intensity from five measurements is recorded for each macro pixel. The spectrometer is HR2000+ from Ocean Optics, which covers the range from 190 to 1100 nm with a resolution of 0.66 nm and step size of 0.44 nm.

Once spectra corresponding to all macro pixels are measured, the wavelength range is cropped to reduce computational effort and the intensities are assembled into a 2D array, where one axis represents wavelength and the other axis represents the location of the macro pixel. First, an intensity mask is generated by applying a 1D median filter along the axis of location, which is subtracted from the original array in order to remove the fixed pattern noise of the spectrometer and the intrinsic drift of the supercontinuum laser spectrum. The 2D array is then reshaped into a 3D hyperspectral cube, where two axes represent the position of the macro pixel on the DMD, and one axis represents wavelength. And 2D Wiener filtering is applied to each wavelength layer for adaptive noise removal. The filtered hyperspectral cube is denoted H and is reshaped back into a 2D array. After spectra with maximum intensity lower than the predefined threshold are discarded, the rest of the spectra are fitted to a Gaussian peak. All Gaussian peaks are combined into a 2D calibration matrix A, where the row index of A represents the wavelength and the column index of A denotes position of the macro pixel.

B. Calibration Result

During the calibration procedure, a hyperspectral cube H is generated containing measured spectra for all macro pixels of the DMD. By combining the wavelength layers in the cube, the echellogram upon the DMD can be synthesized. As shown in Fig. 10, the actual echellogram is rotated with respect to the simulated result shown in Fig. 6 due to the rotation of the DMD in the alignment process. Although most of the energy is concentrated within the free spectral range of each order, a small part of the energy gets leaked out of the free spectral range. Therefore, for certain wavelengths, the energy gets distributed into two/three different orders/locations. The arc stripe where intensity is slightly reduced in the lower part of the synthesized echellogram might be caused by a groove structure anomaly of the echelle grating. It should be noted that the resolution of the echellogram synthesis is limited by the spectral resolution of the spectrometer. To be more specific, a spectrometer with better spectral resolution is capable of generating a sharper synthesized echellogram. In general, the prism is able to separate the orders well enough as expected and the area of the DMD is fully utilized.

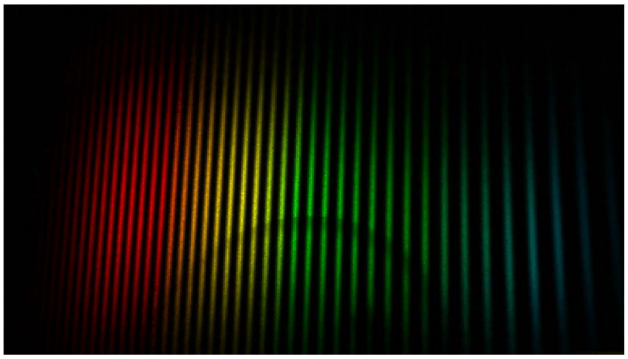

Fig. 10. Synthesized echellogram upon the DMD chip generated from spectral measurements of the scanning macro pixels.

In the calibration procedure, the measured spectral peak of each useful macro pixel (maximum intensity larger than the predefined threshold) is fitted to a Gaussian to reduce the noise in the signal. In Fig. 11, the relationship between the FWHM and the peak wavelength of the fitted Gaussian is illustrated by plotting the fitting result of each macro pixel as a dot. The average FWHM of the fitted Gaussians is 1.02 nm, which indicates that the calibration resolution is very likely limited by the spectral resolution of the spectrometer (approx. 0.66 nm) as well as its pitch size (0.44 nm). Therefore, the actual peak width of the spectrum corresponding to one macro pixel is potentially smaller than the currently measured value.

The amplitude of the fitted Gaussian peaks is also plotted in Fig. 12. Certain periodic variation of the maximum amplitude can be observed from the figure. This is due to the fact that not

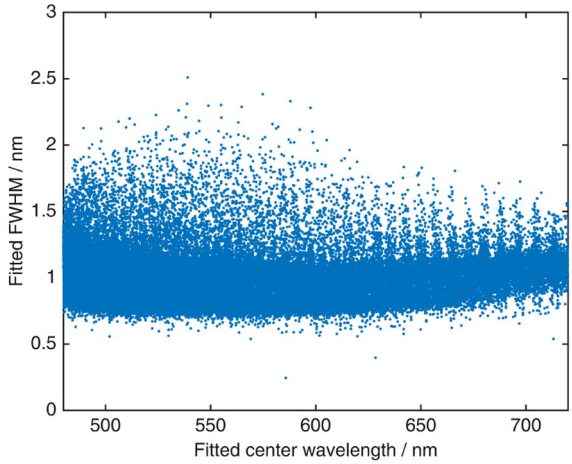

Fig. 11. FWHM with respect to center wavelength of the fitted Gaussian peaks. Measurements corresponding to 54,338 macro pixels are drawn.

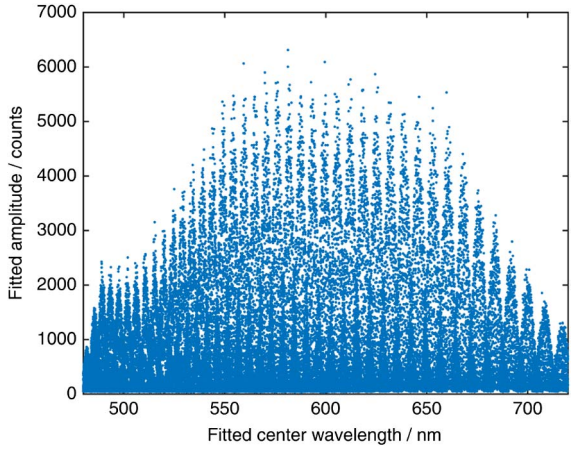

Fig. 12. Amplitude with respect to center wavelength of the fitted Gaussian peaks. Measurements corresponding to 54,338 macro pixels are drawn.

all energy is concentrated within the free spectral range of each order. For the wavelength at the center of the free spectral range of one diffraction order, most energy is concentrated in the corresponding macro pixel, thus achieving higher maximum amplitude for the fitted Gaussian. For the wavelength at the edge of the free spectral range, part of the energy will be distributed to the adjacent order, making the maximum amplitude for this wavelength lower.

To evaluate the effect of the calibration, especially the fitting process, all fitted Gaussian signals of the useful macro pixels are summed and compared against the total spectrum measured when all pixels are turned on. The total spectrum is measured using a much smaller integration time in order to avoid saturation of the spectrometer, and is therefore scaled according to the ratio of integration times. As can be seen in Fig. 13, the sum of the selected macro pixels is quite close to the spectrum when all pixels are turned on. In fact, only 22% of the macro pixels are selected for calibration, which contributes to the majority of the energy, whereas the rest of the pixels are discarded for their poor signal-to-noise ratio.

C. Spectra Generation

The most rigorous way of computing one DMD pattern for the generation of a certain spectrum is by solving the following nonnegative least squares problem:

$$\begin{aligned} &\text{minimize} && |A\mathbf{x} - \mathbf{b}|^2 \\ &\text{subject to} && \mathbf{x} \geq \mathbf{0}, \end{aligned} \tag{4}$$

where $\mathbf{x}$ represents the pattern to be retrieved, A stands for the calibration matrix acquired previously, and $\mathbf{b}$ denotes the target spectrum. Nevertheless, solving the problem with optimization algorithms can be very time consuming, especially considering the size of the calibration matrix.

Therefore, the condition of nonnegativity is ignored and the problem is transformed into the following:

$$\begin{aligned} &\text{minimize} && |\mathbf{x}|^2 \\ &\text{subject to} && A\mathbf{x} = \mathbf{b}, \end{aligned} \tag{5}$$

which attempts to find the least squares solution with minimized norm. The solution can be easily calculated by applying the pseudo-inverse matrix of A to both sides of the linear equation,

$$\mathbf{x}^* = A^{-1}\mathbf{b} = A^T(AA^T)^{-1}\mathbf{b}. \tag{6}$$

Since the FWHM of the fitted Gaussian in the calibration matrix is very narrow, the row rank of the calibration is very close to full. Therefore, the solution by applying the pseudo-inverse matrix tends to be nonnegative in most of the cases. In rare circumstances where the pattern has negative values, the negative values are clipped to zero. As the pseudo-inverse matrix can be calculated off-line and pattern generation requires only one matrix multiplication, this method is much faster than solving the nonnegative least squares problem rigorously with optimization and still provides acceptable results.

Once the pattern is calculated, it is reshaped into the complete DMD size and quantized into 8-bit, which can be displayed through time multiplexing. DMD patterns for several target spectra are calculated and the generated spectra are measured with an integration time of 5 ms.

Figure 14 illustrates the generation of a flat spectrum spanning across the range from 480 to 700 nm. Although with some variation of the intensity due to intrinsic spectral variation of the supercontinuum laser and noise, the generated spectrum is very close to the target. The overshoot on the edges of the flat spectrum can be explained by the Gibbs phenomenon, as the maximum frequency that the system is capable of generating is dependent on the FWHM of the fitted Gaussian for each macro pixel.

Figure 15 demonstrates two ramp spectra from 480 to 680 nm. Similar to the flat spectrum, overshoot can be observed during abrupt change at the edges while the rest of the spectra closely reproduce the targets.

Last but not least, Fig. 16 shows a Gaussian spectrum centered at 580 nm with a FWHM of 10 nm. Gaussian peaks with a narrower FWHM can be generated as well and the smallest possible FWHM is limited by the FWHM of the spectrum generated by a single macro pixel. As mentioned previously, the average FWHM of the fitted Gaussian for each macro pixel is 1.02 nm, which is very likely limited by the resolution of the spectrometer in the current calibration setup.

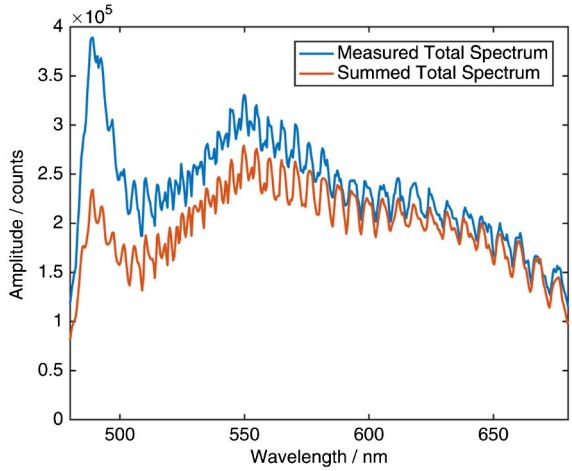

Fig. 13. Comparison between measured total spectrum and calculated spectrum by summing all useful macro pixels.

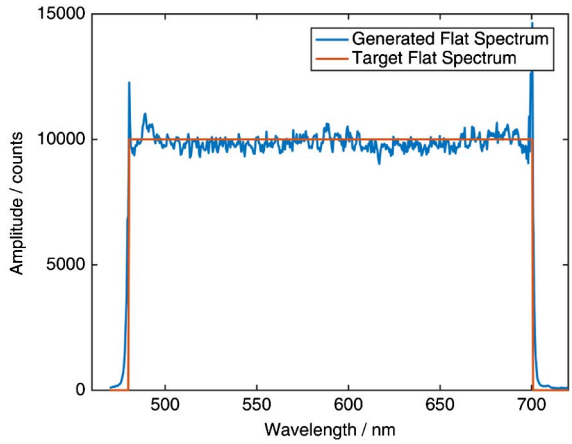

Fig. 14. Comparison between measured flat spectrum and target spectrum.

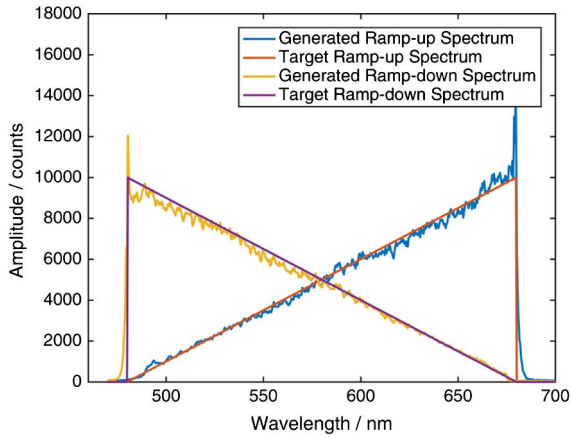

Fig. 15. Comparison between measured ramp spectra and target spectra.

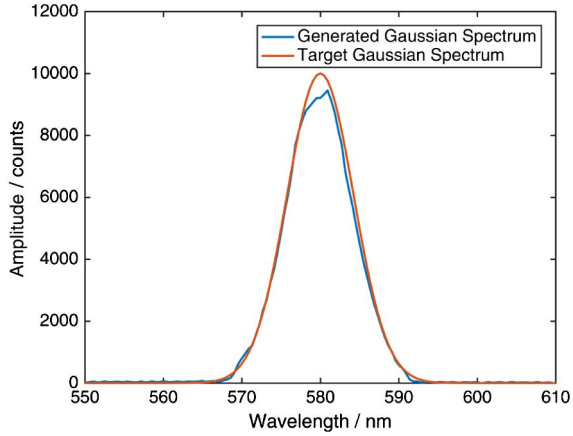

Fig. 16. Comparison between measured Gaussian spectrum and target Gaussian spectrum.

D. Wavelength Tuning Resolution

As the spectrum of the system can be programmed arbitrarily, the combination of the echelle grating and the DMD can also be treated as a tunable band-pass filter, achieving function similar to an acousto-optic tunable filter (AOTF), which is often applied to the supercontinuum laser to realize wavelength scanning.

To characterize the wavelength tuning resolution of the current system, a series of Gaussian spectra are generated, each having a FWHM of 2 nm. The center wavelength of these spectra ranges from 560 to 580 nm with a step size of 0.01 nm. The calibration setup mentioned previously is used to record the generated spectra with an integration time of 5 ms. Gaussian fitting is then applied to all recorded spectra to yield measured center wavelengths, which are compared against the target. As shown in Fig. 17, the measured scanning results demonstrate superior linearity with very few errors. When zoomed into a smaller region of 0.2 nm, it can be seen that a step size of 0.01 nm can be correctly reflected by the

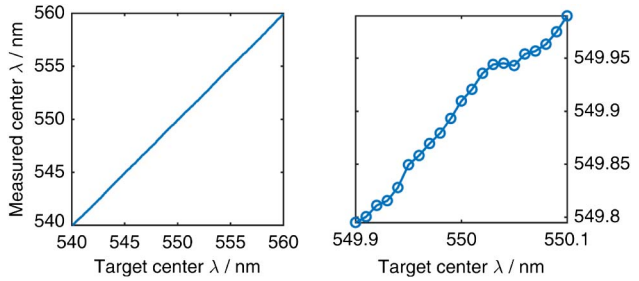

Fig. 17. Scanning of Gaussian spectra with FWHM of 2 nm. Left: wavelength range from 540 to 560 nm. Right: zoomed wavelength range from 549.9 to 550.1 nm.

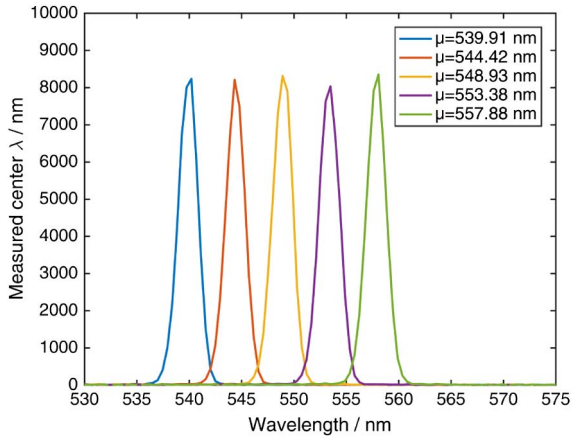

Fig. 18. Five Gaussian spectra from the scanning sequence. Letter μ represents the fitted center wavelength.

measurement with minor errors caused mainly by noise. As an example, Fig. 18 illustrates five measured spectra from the scanning sequence.

5. CONCLUSION

In this paper, a novel programmable light source in the visible range is proposed, which utilizes a supercontinuum laser as the primary source and combines its echellogram with a digital mirror device for programmable spectral filtering. The echellogram is first designed in sequential mode of OpticStudio to have diffraction-limited telecentric imaging upon the DMD. Then the complete system, including the DMD and the coupling of the output light into a liquid light guide, is simulated in non-sequential mode with ray tracing to generate an echellogram image showing the free spectral range of diffraction orders No. 78 to No. 119.

The system is constructed in the lab and evaluated. To calibrate the programmable filter, the output of the liquid light guide is homogenized and projected onto a fiber spectrometer. Pixel blocks of 5×5 are scanned while their corresponding spectral responses are recorded. The recorded data are cleaned, smoothed, and fitted with several processes before the calibration matrix is constructed by assembling fitted Gaussian spectra of the useful macro pixels. Average FWHM of the fitted

Gaussians is 1.02 nm, which is believed to be limited by the resolution and pitch size of the spectrometer. During the calibration procedure, intensity measurements of different wavelengths can be combined to synthesize the echellogram upon the DMD. Two major differences are observed between the measured echellogram and the simulated result from ray tracing. First, a small part of the energy gets leaked out of the free spectral range of each order due to imperfect blazing structure of the echelle grating dependent on the manufacturing accuracy. Second, the width of each order is widened compared to the simulated results, since the ray tracing simulation does not take into account the diffraction limit, as is illustrated in Fig. 3.

Several exemplary spectra are generated and compared against the target, which demonstrates that the spectral filtering is relatively accurate. A series of Gaussian spectra are generated and measured to investigate the wavelength tuning resolution of the system when operated as a scanning source. Results have shown that the system is responsive to a step size of 0.01 nm.

Currently, three major factors are limiting the performance of the system. First, the supercontinuum laser, which is used in the system as the primary input to the programmable spectral filtering system, has a limited spectral stability. On one hand, the intrinsic spectral variation of the supercontinuum laser gets directly passed to the final output. On the other hand, as the calibration process takes a relatively long period of time, the spectral variation is also transferred into the calibration matrix, reducing its accuracy. Second, like most echellogram systems, the programmable filtering setup is very sensitive to mechanical vibrations, since tiny movement of the echelle grating shifts wavelengths by multiple pixels. Currently Sorbothane feet are attached to the breadboard to absorb vibration. Nevertheless, an optical table with active self-leveling isolators would definitely enhance the stability of the system. Last but not least, resolution and pitch size of the USB fiber spectrometer are limiting the calibration accuracy. A spectrometer with less measurement range but higher resolution would be more suitable for the calibration task.

In conclusion, the proposed system is potentially useful for any optical applications where manipulation of the wavelength is necessary. In particular, the system provides a versatile prototyping platform for measurement systems based on the chromatic principle as well as hyperspectral imaging technologies.

Funding. Baden-Württemberg Stiftung gGmbH.

REFERENCES

1. K. Hirai, D. Irie, and T. Horiuchi, "Multi-primary image projector using programmable spectral light source," J. Soc. Inf. Disp. **24**, 144–153 (2016).
2. S. H. Huang, X. Y. Zou, S. M. Hwang, A. E. Willner, Z. Bao, and D. A. Smith, "Experimental demonstration of dynamic network equalization of three 2.5-Gb/s WDM channels over 1000 km using acoustooptic tunable filters," IEEE Photon. Technol. Lett. **8**, 1243–1245 (1996).
3. L. Bei, G. I. Dennis, H. M. Miller, T. W. Spaine, and J. W. Carnahan, "Acousto-optic tunable filters: fundamentals and applications as applied to chemical analysis techniques," Prog. Quantum Electron. **28**, 67–87 (2004).
4. J. Sapriel, D. Charissoux, V. Voloshinov, and V. Molchanov, "Tunable acoustooptic filters and equalizers for wdm applications," J. Lightwave Technol. **20**, 892–899 (2002).
5. M. C. Parker, A. D. Cohen, and R. J. Mears, "Dynamic digital holographic wavelength filtering," J. Lightwave Technol. **16**, 1259–1270 (1998).
6. J. S. Patel and M. W. Maeda, "Tunable polarization diversity liquid-crystal wavelength filter," IEEE Photon. Technol. Lett. **3**, 739–740 (1991).
7. T. Inui, T. Komukai, and M. Nakazawa, "Highly efficient tunable fiber bragg grating filters using multilayer piezoelectric transducers," Opt. Commun. **190**, 1–4 (2001).
8. Y. Ding, M. Pu, L. Liu, J. Xu, C. Peucheret, X. Zhang, D. Huang, and H. Ou, "Bandwidth and wavelength-tunable optical bandpass filter based on silicon microring-MZI structure," Opt. Express **19**, 6462–6470 (2011).
9. N. A. Riza and S. Sumriddetchkajorn, "Digitally controlled fault-tolerant multiwavelength programmable fiber-optic attenuator using a two-dimensional digital micromirror device," Opt. Lett. **24**, 282–284 (1999).
10. N. A. Riza and M. J. Mughal, "Broadband optical equalizer using fault-tolerant digital micromirrors," Opt. Express **11**, 1559–1565 (2003).
11. C. H. Chuang and Y. L. Lo, "Digital programmable light spectrum synthesis system using a digital micromirror device," Appl. Opt. **45**, 8308–8314 (2006).
12. T. C. Wood and D. S. Elson, "A tunable supercontinuum laser using a digital micromirror device," Meas. Sci. Technol. **23**, 105204 (2012).
13. Y. Soskind, *Field Guide to Diffractive Optics* (SPIE, 2011).
14. https://zenodo.org/record/15763?ln=en#.WLV-7m8rKU.